ELSEVIER

Journal of Non-Crystalline Solids 299–302 (2002) 678–682

JOURNAL OF NON-CRYSTALLINE SOLIDS

www.elsevier.com/locate/jnoncrysol

Bright luminescence from erbium doped nc-Si/SiO_2 superlattices

M. Schmidt [a,*], J. Heitmann [b], R. Scholz [b], M. Zacharias [b]

[a] *Institut für Experimentelle Physik, Otto-von-Guericke Universität Magdeburg, PF 4120, 39016 Magdeburg, Germany*
[b] *Max-Planck-Institut für Mikrostrukturphysik, Weinberg 2, 06120 Halle, Germany*

Abstract

Optical properties of Er doped Si/SiO_2 superlattices and SiO/SiO_2 superlattices are compared. In the case of Si/SiO_2 superlattices with Si layers thicknesses between 2 and 19 nm polycrystalline like Si layers are observed after annealing. The samples show a very weak defect related red room temperature luminescence. No significant enhancement of the Er luminescence could be shown. The SiO/SiO_2 superlattices show after annealing the evidence of separated Si nanocrystals and a very strong red room temperature luminescence. The emission wavelength varies between 750 and 850 nm depending on the SiO layer thickness. In this case, a strong enhancement of the Er^{3+} luminescence by more than one order of magnitude was observed. Temperature dependent photoluminescence (PL) measurements of the 1.54 μm Er^{3+} luminescence are included.

PACS: 78.55.−m; 61.72.Tt; 61.46.+w

1. Introduction

Er doped silicon has attracted particular attention because the Er^{3+} transition $^4I_{13/2} \rightarrow {}^4I_{15/2}$ at 1.54 μm matches the minimum in absorption of silica-based optical fibers. However, the strong thermal quenching behavior of Er doped crystalline Si on going from He to room temperature limits or even prevents the application of Si:Er in optoelectronic devices. Kik et al. [1] reported an intensity quenching by more than a factor of thousand upon increasing the temperature from 12 to 150 K. The incorporation of impurities, first of all oxygen, can significantly increase the luminescence intensity [2,3]. It has been shown that impurities may affect the segregation of Er indicating that the presence of oxygen dramatically reduces the segregation of Er in crystalline Si. EXAFS measurements on Er and O co-implanted Si demonstrated that Er forms complexes with oxygen coordinated by four or six O atoms [4]. The addition of oxygen to Er-implanted CZ–Si enhances the photoluminescence (PL) intensity which is, at least partly, attributed to the increase in the density of O-coordinated and therefore optical active Er. In addition, oxygen implantation also reduces the PL quenching at elevated temperature. It is assumed that the Er–O complex provides a defect

* Corresponding author. Tel.: +49-391 67 12361; fax: +49-391 67 11130.
E-mail address: m.schmidt@student.uni-magdeburg.de (M. Schmidt).

0022-3093/02/$ - see front matter
PII: S0022-3093(01)01031-6

level in the Si band. An electron may be trapped at the defect and a hole may be subsequently be bond forming a bond electron–hole complex. If this electron–hole pair recombines in the vicinity of Er, the energy may be transferred through an Auger process or due to dipole–dipole coupling to the Er^{3+} ion which becomes excited and can decay by the emission of a 1.54 μm photon. However, the bond electron–hole complexes may dissociate before the energy is transferred to the Er or the Er ion decays by a non-radiative process. Both quenching processes require annihilation of one or more phonons which becomes more probable at higher temperature [3].

Room temperature luminescence of the Er intra-4f transition can only be achieved if sufficient Er can be brought into the first excited state. Because the optical cross-section for the intra-4f transition is typically on the order of only 10^{-21} cm^2 there is considerable interest in sensitizing the Er^{3+} ions by adding a strongly absorbing material that can transfer the energy efficiently to Er. Recently, it was reported that the presence of Si nanocrystals in Er doped SiO_2 effectively enhances Er luminescence [5,6]. As a model, it was suggested that light is absorbed within the Si nanocrystals resulting in confined e–h pairs. An energy transfer either by an Auger process or by dipole–dipole coupling mediates than the excitation of the Er^{3+} ions.

Samples containing Er and Si nanocrystals were prepared by reactive evaporation [7] or co-sputtering [8]. A dense and ordered arrangement of the Si nanocrystals can be realized using this methods to produce nanocrystalline Si/SiO_2 [8] or SiO/SiO_2 superlattices [9,10]. This work is focused on the optical properties of the Er doping of such nanocrystalline Si/SiO_2 superlattice.

2. Experimental

Two different sample series were prepared. Sample series A: amorphous Si/SiO_2 superlattices were prepared by rf sputtering and plasma oxidation [8]. The Si layer thickness varies between 2.2 and 19 nm. Er ions were implanted at 250 keV with a dose of 4×10^{14} cm^{-2}. Rapid thermal annealing (RTA) was done for 1 min at 900 °C to initiate nucleation seeds in the amorphous Si layers. Conventional furnace annealing at 800 °C for times between 5 and 25 min was carried out to complete the crystallization as well as to heal the implantation damage.

Sample series B consists of samples with amorphous SiO/SiO_2 superlattices. These samples were prepared by reactive evaporation of SiO and SiO_2 alternately [9,10]. The SiO layer thickness varies between less than 1 and 3 nm. The number of periods varies between 45 and 90 for different samples. Conventional furnace annealing at 1100 °C under N_2-atmosphere for 1 h was carried out. Er ions were implanted at 300 keV with a dose of 5×10^{14} cm^{-2}. After the Er implantation RTA at 950 °C for 5 min was done. For comparison the same Er dose was implanted in a thick SiO_2 film, evaporated under the same conditions.

For high resolution transmission electron microscopy measurements (HRTEM), cross-section samples were prepared in the usual way including final Ar ion milling. The investigations were performed under high resolution imaging conditions at a JEM-4010 electron microscope (400 kV, point resolution 0.16 nm). The PL was measured using an Ar ion laser at 488 nm as excitation source. The used excitation power was below 150 mW. The PL was focused on the entrance of a 50 cm monochromator and detected by a LN cooled Ge detector and a CCD array. All spectra are corrected by spectral response of the measurement system. The temperature dependent PL measurements in the region from 300 K down to 5 K were performed using a He bath cryostat.

3. Results

Fig. 1 shows the HRTEM images of two samples of sample series A (a) with 7.3 nm Si layer thickness, (b) 2.2 nm Si layer thickness and of a sample of series B (c) with 3 nm thick SiO layers after annealing. In the case of the Si/SiO_2 superlattices (series A) the 7 nm thick Si layers are fully crystallized in randomly oriented Si nanocrystals. The layers containing nanocrystals are clearly separated by the thin 4.5 nm SiO_2 sublayers. The

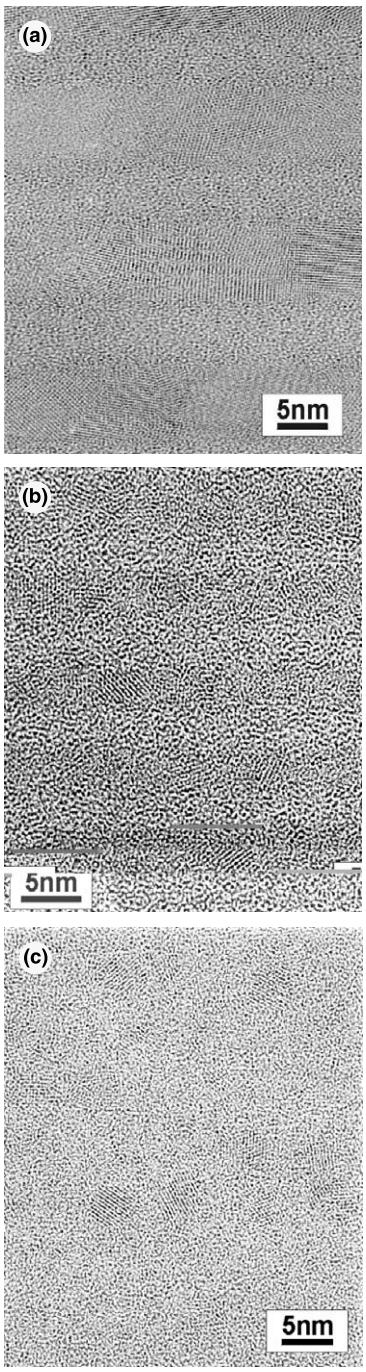

Fig. 1. HRTEM images of: (a) a Si/SiO_2 superlattice with a Si layer thickness of 7.3 nm, (b) a Si/SiO_2 superlattice with a Si layer thickness of 2.2 nm, (c) of the SiO/SiO_2 superlattices with a SiO layer thickness of 3 nm after crystallization.

crystals within one layer touch each other and forms a multicrystalline Si layer. The average Si crystal size is 5.3 ± 0.7 nm extracted by X-ray diffraction analysis (XRD) [11]. For thinner Si layer thickness (Fig. 1(b)) some of the crystals seems to be separated with an average crystal size of 2.7 ± 0.5 nm [11]. The HRTEM investigation at the sample of series B with an SiO layer thickness of 3 nm shows isolated Si nanocrystals embedded in the SiO_2 matrix. The nanocrystal average diameter extracted for this sample is 3.5 ± 0.5 nm. By XRD the average nanocrystal size was estimated using the Scherrer equation to be 3.4 ± 0.5 nm.

The PL spectra in the visible region of sample set A are shown in Fig. 2. The PL spectra for samples series A show main maxima at 650 and at 750 nm. There is no evident correlation between Si layer thickness and PL emission wavelength or intensity. In contrast, sample series B shows a very intense quantum confinement originated NIR-PL signal with a clear correlation between crystal size and PL peak position. The emission wavelength varies from 890 nm for the sample with an SiO layer thickness of 3–750 nm for the sample with an SiO layer thickness of less than 1 nm [10]. After Er doping sample series A shows Er^{3+} luminescence at 1.54 μm with a weak intensity which is independent from Si layer thickness (Fig. 2(b)). The sample with the smallest Si layer thickness (2.2 nm) shows the most intense Er luminescence.

Fig. 3 shows the comparison of the Er^{3+} luminescence of a sample with a Si layer of 2.2 nm thickness from sample series A, the sample with SiO layer thickness of 3 nm of series B and Er implanted pure SiO_2 for the same Er dose (5×10^{14} cm^{-2}) after annealing. The sample of series B shows a 25 times enhanced Er^{3+} PL intensity.

Fig. 4 compares the temperature dependence of the PL signal of the Er doped SiO/SiO_2 superlattices of different layer thickness and the Er doped thermal oxide sample. The observed thermal degradation is below one order of magnitude and similar for the superlattices with different layer thicknesses but noticeable different from the Er doped oxide. For all investigated samples of series B an enhancement of the Er^{3+} luminescence by factor between 20 and 40 over the whole temperature range is observable.

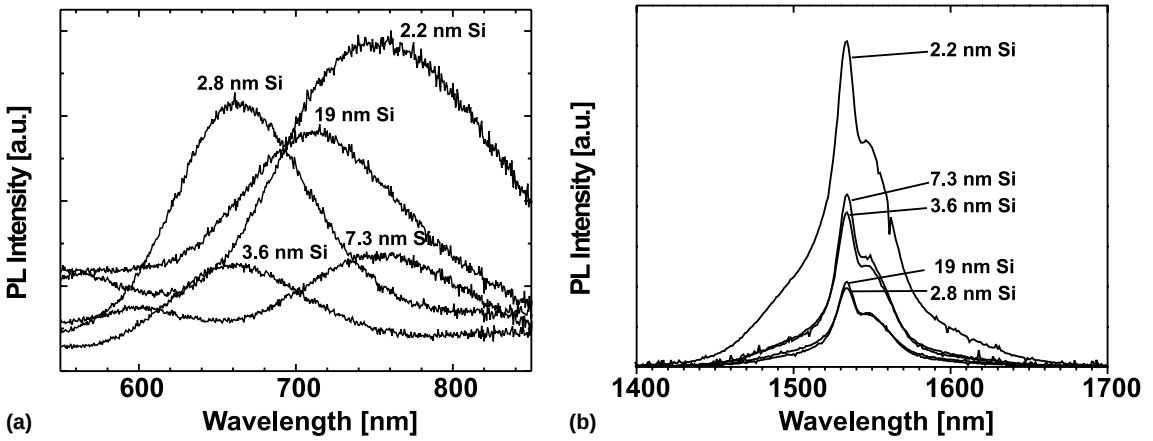

Fig. 2. Photoluminescence spectra in the (a) visible and (b) infrared region for different Si layer thicknesses of the Si/SiO_2 superlattices.

4. Discussion

From HRTEM images it is proven that the main difference between sample series A and B is the occurrence of mainly polycrystalline Si layers in samples of series A and isolated Si nanocrystals in an SiO_2 matrix in series B. In the case of sample series B the nanocrystals are the product of a thermal induced phase separation of SiO in SiO_2 and Si nanocrystals [7]. The superlattice arrangement gives a control over the Si nanocrystal size [9,10]. This explains the differences observed in the PL behavior. The Si layer thickness independent emission wavelength of the PL signal of series A at 650 and 750 nm and the very weak PL intensity indicate defects at the nc-Si/nc-Si interfaces or in the oxide matrix itself as origins of this luminescence. In the case of evaporated and phase separated thick SiO_x films Kahler and Hofmeister [7] suggested the quantum confinement model as origin of the strong room temperature luminescence and showed Si phonon replica in the resonant excited PL signal. This is in agreement to our observed strong room temperature PL signal and

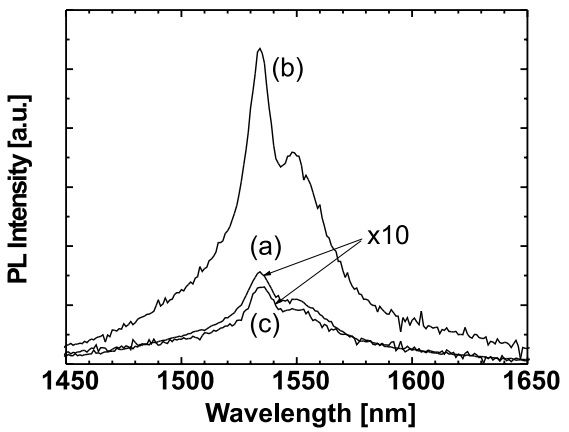

Fig. 3. Room temperature PL of Er doped (a) Si/SiO_2 superlattices, (b) SiO/SiO_2 superlattices, (c) SiO_2 after annealing.

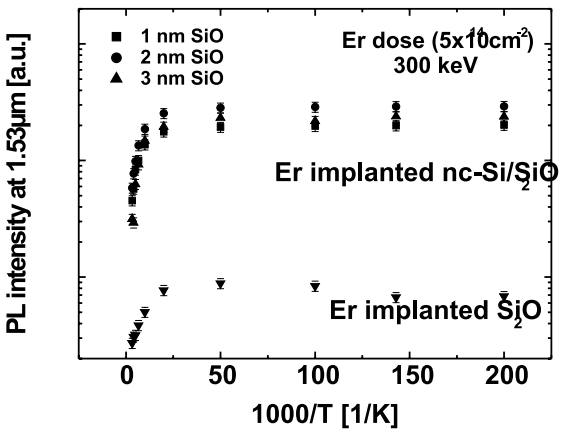

Fig. 4. Temperature dependence of the Er luminescence at 1.54 μm of the SiO/SiO_2 with SiO layer thicknesses between 1 and 3 nm.

the shown blue shift with decreasing SiO layer thickness [10]. Only for samples of series B a significant enhancement of the Er^{3+} luminescence is observable. We conclude that the preparation of a dense matrix of isolated Si nanocrystals showing a high PL intensity due to quantum confinement is one of the key elements for a high intensity of the Er luminescence. A nanocrystal size dependent effect of the Er^{3+} luminescence enhancement could not be shown so far, but is still under investigation. In case of the Si/SiO_2 superlattices the Si layers can be more described as polycrystalline films with dangling bonds and other surface defects at the grain boundaries of the adjacent nanocrystals and non radiative processes in abundance. Therefore, neither quantum confinement based Si luminescence nor an enhancement of the Er^{3+} PL intensity is observed. The higher luminescence intensity of the sample with the thinnest Si layer thickness (2.2 nm) points out that for very thin silicon layers a synthesis of separated Si nanocrystals should be possible as proven by TEM investigations.

With an Er dose of 5×10^{14} cm^{-2} we are still far away from where a segregation of Er into clusters is expected and which would result in an optical inactive state of the Er. Also this Er dose is too low to consume all the photons emitted from the Si nanocrystals by the Er excitation path which means that the Si emission output is decreased but not depleted as shown for similar systems [6,12].

The thermal degradation of the Er luminescence is comparable to values reported for SiO_2 containing random distributed Si nanocrystals [5,6] which indicates a comparable radiative processes for both of these systems.

5. Conclusion

In conclusion, the properties of Er doped Si/SiO_2 superlattices and SiO/SiO_2 superlattices were investigated. Layer-arranged Si nanocrystals were observed by high resolution transmission electron microscopy. The key point for a high PL intensity of the ordered arranged Si nanocrystals and the correlated enhancement of the Er luminescence is the separation of the Si nanocrystals by a thin SiO_2 barrier. We found that a sufficient number of Si nanocrystals are clearly separated only in SiO/SiO_2 superlattices. In this case, an enhancement of the Er^{3+} luminescence by more than one order of magnitude was observed. In the case of Si/SiO_2 superlattices the annealing procedure results in polycrystalline Si layers which show neither strong room temperature luminescence of the Si nanocrystals nor a significant enhancement of the Er^{3+} luminescence.

Acknowledgements

The authors gratefully acknowledge G. Lenk from Friedrich–Schiller–University Jena for the ion implantation of the samples. This work has been financially supported by Volkswagen Stiftung.

References

[1] P.G. Kik, M.J.A. de Dood, K. Kikoin, A. Polman, Appl. Phys. Lett. 70 (1997) 1721.
[2] J. Michel, J.L. Benton, R.F. Ferrante, D.C. Jacobson, D.J. Eaglesham, E.A. Fitzgerald, Y.-H. Xie, J.M. Poate, L.C. Kimerling, J. Appl. Phys. 70 (1991) 2672.
[3] A. Polman, J. Appl. Phys. 82 (1997) 1.
[4] D.L. Adler, D.C. Jacobsen, D.J. Eaglesham, M.A. Marcus, J.L. Benton, J.M. Poate, P.H. Citrin, Appl. Phys. Lett. 61 (1992) 2182.
[5] M. Fujii, M. Yoshida, Y. Kanzawa, S. Hayashi, K. Yamamoto, Appl. Phys. Lett. 71 (1997) 1198.
[6] M. Fujii, M. Yoshida, S. Hayashi, K. Yamamoto, J. Appl. Phys. 84 (1998) 4525.
[7] U. Kahler, H. Hofmeister, Opt. Mater. 17 (2001) 83.
[8] M. Zacharias, J. Bläsing, P. Veit, L. Tsybeskov, K.D. Hirschman, P.M. Fauchet, Appl. Phys. Lett. 74 (1999) 2614.
[9] M. Zacharias, J. Heitmann, R. Scholz, U. Kahler, M. Schmidt, J. Bläsing, Appl. Phys. Lett. 80 (2002) 661.
[10] J. Heitmann, R. Scholz, M. Schmidt, M. Zacharias, these Proceedings, p. 1075. Solids (ICAMS 2001), submitted.
[11] M. Schmidt et al., Thin Solid Films 397 (2001) 211.
[12] M. Zacharias, J. Heitmann, M. Schmidt, P. Streitenberger, Physica E 11 (2001) 245.